Nuclear Imaging Probes: from Bench to Bedside

Hans-Jürgen Wester

Abstract The availability of specific imaging probes is the nuclear fuel for molecular imaging by positron emission tomography and single-photon emission computed tomography. These two radiotracer-based imaging modalities represent the prototype methods for noninvasive depiction and quantification of biochemical processes, allowing a functional characterization of tumor biology. A variety of powerful radiolabeled probes—tracers—are already established in the routine clinical management of human disease and others are currently subject to clinical assessment. Emerging from investigations of the genomic and proteomic signatures of cancer cells, an increasing number of promising targets are being identified, including receptors, enzymes, transporters, and antigens. Corresponding probes for these newly identified targets need to be developed and transferred into the clinical setting. Starting with a brief summary of the characteristics and prerequisites for a "good tracer," an overview of tracer concepts, target selection, and development strategies is given. The influence of the imaging concepts on tracer development is also discussed.

The term "molecular imaging," currently defined as "*in vivo* imaging of biological or biochemical processes," originally describes the visualization of a target molecule *in vivo* by virtue of its interaction with a probe at the molecular level. In recent years, the field of molecular imaging has broadened and includes several different modalities [e.g., nuclear imaging, magnetic resonance imaging, magnetic resonance spectroscopy, computed tomography (CT), ultrasound, bioluminescence, and fluorescence imaging; ref. 1]. Among these modalities, nuclear molecular imaging with positron emission tomography (PET) and single-photon emission CT represent the prototype for noninvasive quantitative tracing of biochemical processes *in vivo*. A radiolabeled compound is applied to follow a pathway (transport rate, binding capacity, metabolic rate, etc.) and to detect the utilization of an endogenous analogue (ion, substrate, hormone, etc.) or the expression pattern and density of its corresponding biochemical counterpart (transporter, receptor, enzyme, etc.). To avoid any disturbance of the biochemical or kinetic equilibrium of the process being studied, no-carrier-added tracer preparations without macroscopic or pharmacologic amounts of the respective nonlabeled analogue are applied. A radiopharmaceutical administered at the tracer (no carrier added) level will optimally reach concentrations at the target site *in vivo* in the picomolar to femtomolar range. According to the law of mass action, binding of a compound in such a low concentration to a target structure (e.g., a receptor) requires a binding affinity constant (K_a) in the high picomolar to low nanomolar range. Assuming that the molecular target relevant to the disease of interest is differentially overexpressed and accessible for the probe, the signal "detected by PET" provides a tomographic (three dimensional), quantitative data set of the target distribution and density. In addition, using sophisticated tracer kinetic modeling, kinetic variables, such as equilibrium or flux constants, can be calculated.

The nuclear tracer technique in combination with PET imaging has advanced the functional evaluation of cancer *in vivo*. 2-[^{18}F]fluoro-2-deoxy-D-glucose ([^{18}F]FDG; Fig. 1) constitutes a large part of the success story of PET and is extensively used for diagnosis, staging, and therapy control of cancer. But other radiopharmaceuticals, addressing proliferation, hypoxia, angiogenesis, apoptosis, receptor expression, metastasis, or gene transfection, have also been established in part in the clinic (2) and continue to be developed in preclinical and clinical studies (Fig. 2).

Key Steps in the Development of Nuclear Probes

The development of a probe for nuclear molecular imaging requires the following key questions to be addressed. (*a*) Is the target specific for the disease of interest and can it be relevantly addressed by a radiolabeled probe? To provide a functional characterization of a disease process, the target density, and thus the tracer uptake, has to be representative of the extent and progression of the disease. (*b*) Is there existing a molecule (e.g., an enzyme, receptor ligand, peptide, or antibody) with relevant target affinity and suitability to serve as a lead for the development as a tracer? (*c*) The physiochemical behavior of the tracer *in vivo* should correspond with the half-life of the isotope (e.g., half-life: ^{11}C = 20 min, ^{18}F = 110 min, and ^{68}Ga = 68 min). Is it possible to modify and optimize the lead

Author's Affiliation: Department of Nuclear Medicine, Technische Universität München, Munich, Germany
Received 2/1/07; revised 4/12/07; accepted 4/13/07.
Grant support: Bavarian Ministry of Science, Research and Arts (BayGene).
Requests for reprints: Hans-Jürgen Wester, Department of Nuclear Medicine, Technische Universität München, Ismaninger Strasse 22, 81675 Munich, Germany. Phone: 49-89-41-40-45-86/49-89-41-40-29-73; E-mail: h.j.wester@lrz.tum.de.

doi:10.1158/1078-0432.CCR-07-0264

molecule about radiolabeling strategy, *in vivo* stability, clearance route and kinetics, specificity of binding, and background radioactivity levels? (*d*) Does the tracer accumulation *in vivo* correlate with the biochemical process? This most relevant validation and final preclinical milestone has to be evaluated in suitable animal models, with human tumor xenografts potentially serving as the first relevant proof of the hypothesized target/tracer concept. (*e*) Can the imaging concept developed and validated in animals be translated to man? The validation step in man requires independent assays on tissue samples obtained from biopsies and surgical specimens. Consequently, the transfer of a new nuclear imaging probe from bench to bedside is a complex multidisciplinary process. Some of the issues about the aforementioned questions and concepts for PET tracers are discussed in more detail in this article based in examples of clinical relevancy.

Target Selection

In general, the selection of a target for imaging depends on knowledge of the disease-specific molecular processes that are characteristic for the disease of interest. A pharmacotherapeutic agent needs to inhibit or block targets that are involved in key processes to reach a curative effect (e.g., thymidylate synthase inhibitors, dihydrofolate reductase inhibitors, or tyrosine kinase inhibitors). In contrast, a tracer for diagnostic imaging must bind to the therapeutic target or to a corresponding molecule in the same or downstream metabolic/signaling pathway without initiating a pharmacologic effect. In nearly all cases, a therapeutic target is also suitable for imaging, but the reverse is not necessarily true. Consequently, nuclear medicine can draw extensively on the increasing knowledge generated by genomics and proteomics. Dozens of potential imaging targets have been revealed from a comparison of the different molecular signatures of patients suffering from a given disease compared with those of (healthy) controls (3, 4). Furthermore, the protein expression pattern on tissue samples collected before treatment can be used to identify and select potential therapy responders. Obviously, these evaluations can also be useful for the selection of targets suitable for the prediction of the therapeutic outcome by molecular imaging. However, the current development of nuclear probes is predominantly based on targets and lead structures identified and generated by the pharmaceutical industry. This leads to a bias and an arbitrary restriction ("negative selection") of potential imaging targets because the vast majority of targets that are unsuitable for therapy have thus far not been investigated for molecular imaging purposes.

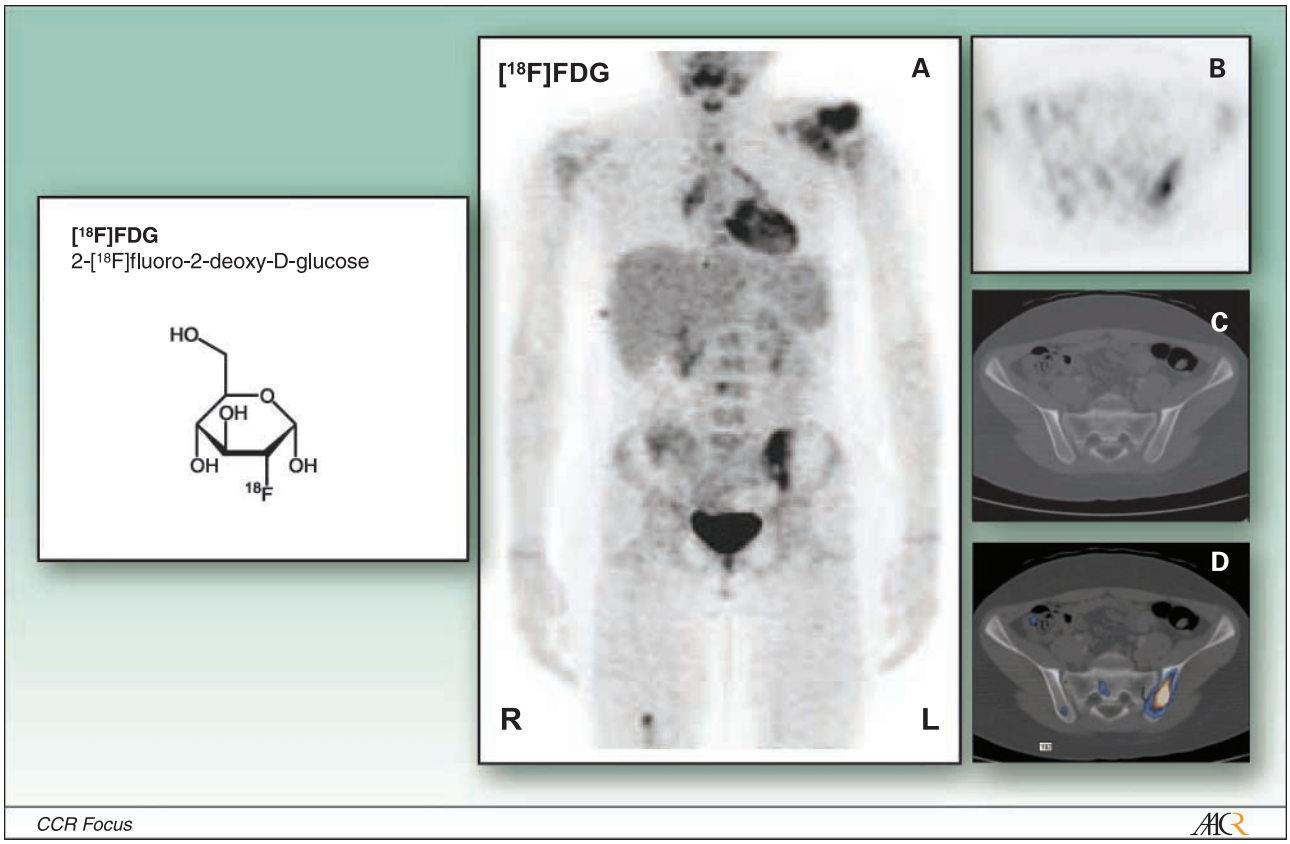

Fig. 1. [^{18}F]FDG. [^{18}F]FDG-PET/CT of a patient with Ewing's sarcoma. The primary tumor is located in the left shoulder region. Intense uptake of FDG can be detected in the primary tumor as well as in multiple bone metastases. *A,* maximum intensity projection of [^{18}F]FDG-PET. *B,* transaxial section of [^{18}F]FDG-PET through the pelvis. *C,* corresponding transaxial section of CT. *D,* fused image ([^{18}F]FDG-PET/CT). Transaxial sections indicate a bone metastasis in the left iliac bone not visible on the corresponding CT section.

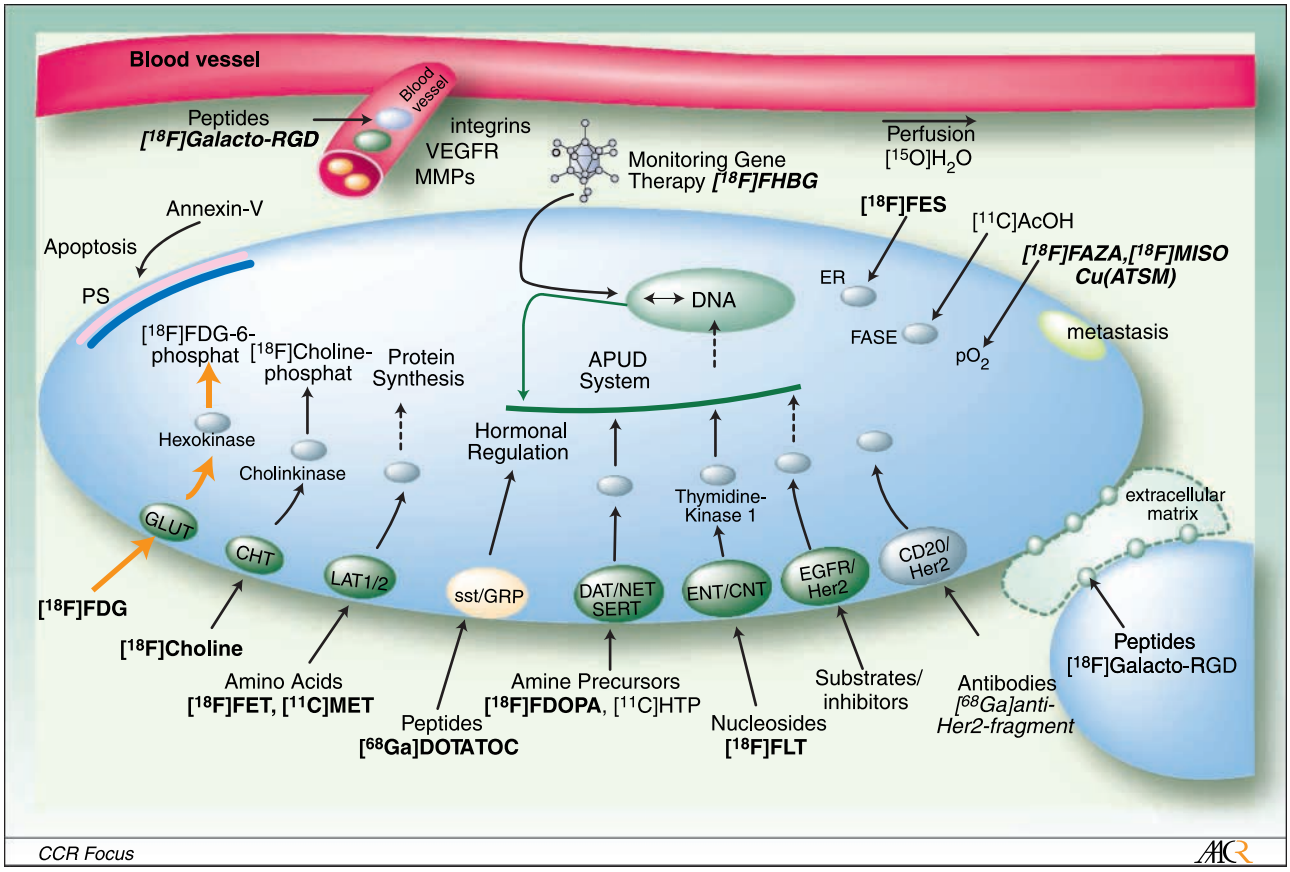

Fig. 2. Selected targets and corresponding nuclear imaging probes already established for nuclear molecular imaging in the clinic (*bold*) or currently under assessment in clinical studies (*italic*).

Probes and Probe Development

Organic synthesis and combinatorial chemistry, solid-phase peptide syntheses, and phage display are techniques generally exploited for generating potential high-affinity binders for a selected target. The combination of quantitative structure-activity relationships and other three-dimensional computational techniques is now standard parts of modern drug design.

Optimization of endogenous ligands is another valuable strategy. Somatostatin receptor 2–binding octapeptides, such as [^{68}Ga]DOTA-D-Phe^{1}-Tyr^{3}-octreotide (5, 6) or Gluc-Lys^{0}-([^{18}F]FP)-Tyr^{3}-octreotide (7, 8), are suitable for imaging of neuroendocrine tumors. Cyclic Arg-Gly-Asp–containing (RGD) pentapeptides such as [^{18}F]Galacto-RGD show high affinity to the $\alpha_v\beta_3$ integrin (9–11). A series of other peptides have been developed that are size-reduced analogues of their endogenous counterparts. They are optimized with respect to their *in vivo* stability, affinity, high specificity of binding, low unspecific uptake, fast excretion via the urinary route, etc. Similarly, small antibody fragments, such as scFv, F(ab')$_2$, or diabodies, are preferred over intact antibodies to overcome their long whole-body residence time and slow excretion (12). For example, the F(ab')$_2$ fragment of the anti-HER2 antibody herceptin is a valuable tracer even when combined with short-lived isotopes, such as ^{68}Ga (half-life of 68 min; ref. 13). Perhaps the most straightforward route to develop a suitable tracer is based on the derivatization or direct labeling of small endogenous molecules, such as the estrogen receptor ligand [^{18}F]fluoro-16α-fluoroestradiol ([^{18}F]FES; refs. 14, 15) or the amino acid transport tracers *O*-(2-[^{18}F]fluoroethyl)-L-tyrosine ([^{18}F]FET) and [^{11}C-methyl]-L-methionine ([^{11}C]MET; refs. 16–18). Both [^{18}F]FET (Fig. 3) and [^{11}C]MET have been established as valuable tracers for imaging of cerebral tumors.

For targeting of intracellular enzymes, radiolabeled substrates lead to high tracer accumulation via a repetitive substrate turnover and trapping. Thus, enzyme amplification of radiotracer accumulation is preferred over radiolabeled probes that bind to target molecules in a 1:1 ratio. The most prominent examples are [^{18}F]FDG as substrate for hexokinase to measure glucose consumption; 3-[^{18}F]fluoro-3-deoxythymidine ([^{18}F]FLT) as a substrate for thymidine kinase 1 to quantify tumor cell proliferation (19, 20); [^{11}C]choline (Fig. 4; refs. 21, 22), [^{18}F]fluoromethyl-choline, and [^{18}F]fluoroethyl-choline (23, 24) as substrates for choline kinase to image prostate carcinomas and other solid cancers; 6-[^{18}F]fluoro-3,4-dihydroxy-L-phenylalanine ([^{18}F]FDOPA) for the detection of neuroendocrine tumors (Fig. 5; ref. 25); and 9-(4-[^{18}F]-fluoro-3-hydroxymethylbutyl)-guanine ([^{18}F]FHBG) for imaging of gene expression (26, 27). Although some extracellular proteases can be imaged

using radiolabeled antibodies, such as ProstaScint imaging of the prostate-specific membrane antigen acting as a glutamate carboxypeptidase (28), targeting of proteases is extremely challenging. All currently known successful trapping mechanisms of small molecules addressing proteases use suicide inhibition and, thus, are not recommended for nuclear imaging. Matrix metalloproteinase (29) and caspase activity (30–32) represent extremely interesting targets, but only a few compounds have been investigated for imaging.

Specific Targets and Imaging Probes

Proliferation. A variety of tracers have been evaluated for imaging of proliferation. ^{11}C-labeled thymidine was the first tracer evaluated and investigated *in vivo*. A major limitation of [^{11}C]TdR is its rapid catabolism (plasma half-life of 3-5 min). This drawback has been overcome with the development of ^{18}F-fluorinated tracers that have better metabolic stability [e.g., 3-[^{18}F]fluoro-3-deoxy-thymidine ([^{18}F]FLT); Fig. 6]. Compared with [^{11}C]thymidine, the phosphorylation rate of [^{18}F]FLT by thymidine kinase 1 is reduced by ~70%. Although triphosphorylation and incorporation of [^{18}F]FLT into the DNA is negligible (<5%), it has been shown that the tracer uptake and monophosphorylation correlates with proliferation rate. [^{18}F]FLT exhibits high *in vivo* stability, which facilitates tracer kinetic modeling, and is becoming accepted for the imaging and quantification of proliferative activity in both animals and patient (33–35). The extent of incorporation into DNA of some newer tracers, such as [^{11}C]FMAU and [^{18}F]BFU, is significantly higher than for [^{18}F]FLT (36), but further investigations are required to determine its effect on signal intensity and the accuracy of proliferation imaging.

Angiogenesis. During the last years, neoangiogenesis has been intensively investigated as a key step in tumorigenesis and as a target for cancer therapy. There is an undiminished interest in developing methods for the noninvasive monitoring of molecular targets involved in angiogenesis, which is further spurred by the need to assess and monitor the effects of new antiangiogenesis-targeted therapies (37).

Currently, the development of angiogenesis-targeted radiotracers is mainly concentrated on peptidic and nonpeptidic $\alpha_v\beta_3$ integrin-binding antagonists, matrix metalloproteinase inhibitors, single-chain antifibronectin antibody fragments, and VEGF-directed tracers (38).

The development of radiolabeled matrix metalloproteinase inhibitors is based either on small organic compounds or the decapeptide Cys-Thr-Thr-His-Trp-Gly-Phe-Thr-Leu-Cys (the latter was obtained from screening of a phage display library;

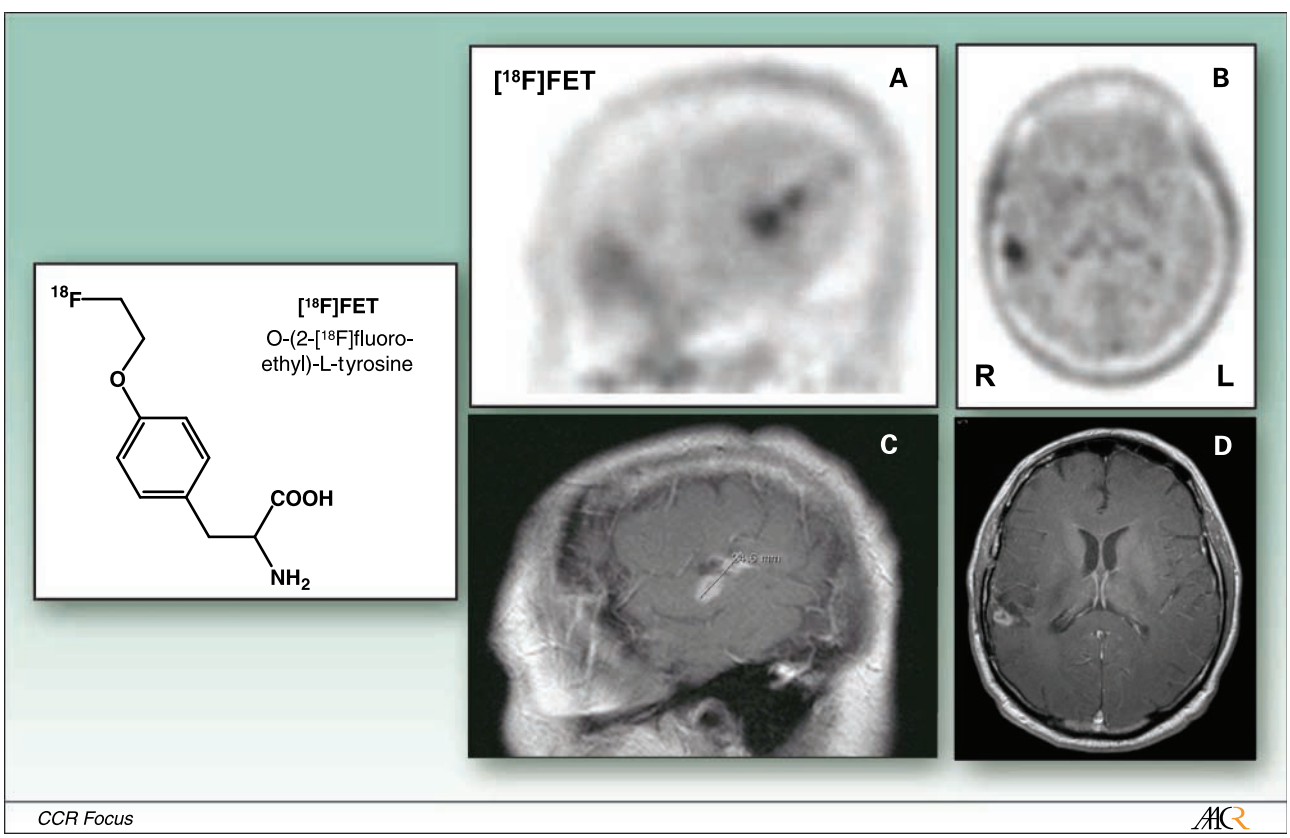

Fig. 3. [^{18}F]FET. [^{18}F]FET-PET of a patient with suspicion of glioblastoma recurrence. Two regions of intense focal uptake in the right temporal lobe, corresponding to the region of contrast agent uptake in the T1 sequence of the magnetic resonance imaging scan, consistent with glioblastoma recurrence. *A,* sagittal section of [^{18}F]FET-PET. *B,* corresponding transaxial section of [^{18}F]FET-PET. *C,* T1 sequence with contrast enhancement (sagittal section) of the corresponding magnetic resonance imaging scan. *D,* T1 sequence with contrast enhancement (transaxial section) of the corresponding magnetic resonance imaging scan.

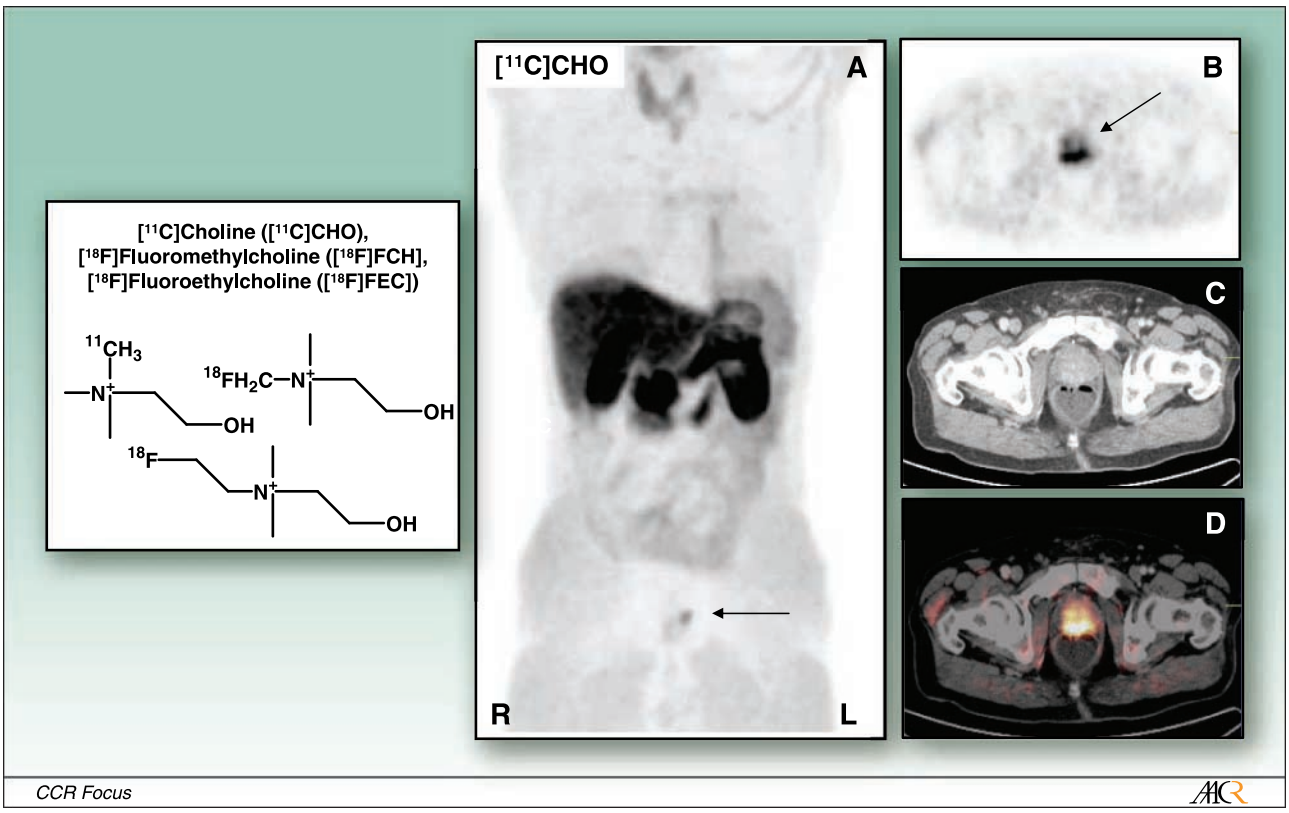

Fig. 4. [^{11}C]Choline. [^{11}C]Choline-PET/CT of a patient with prostate cancer. Intense focal tracer uptake can be detected in the prostate gland. No further radioactivity "hotspots" (lesions) are visualized, indicating no present lymph node or distant metastases. *A,* maximum intensity projection of [^{11}C]choline-PET. *B,* transaxial section of [^{11}C]choline-PET. *C,* corresponding transaxial section of CT. *D,* fused image ([^{11}C]choline-PET/CT).

see ref. 29 and references therein). Although the *in vitro* data for some of these tracers are very promising, more detailed *in vivo* studies have to show the potential of matrix metalloproteinase inhibitors for *in vivo* imaging.

The radiolabeled anti-ED-B single-chain antibody fragment scFv L-19 showed selective accumulation in the tumor vasculature in a murine tumor model. In the first patient study, a selective localization of the radioiodinated tracer in lesions of different tumors was found. A labeled S-S-dimeric recombinant protein AP39, an engineered derivative of L-19, showed very promising biodistribution and imaging properties in mice with a high and rapid tumor uptake, rapid blood clearance, and pronounced renal excretion, leading to high signal-to-noise (target to background) ratios (39–41).

Radiolabeled peptides based on the lead structure cyclo(-Arg-Gly-Asp-DPhe-Val) [=c(RGDfV)] have been developed for the noninvasive determination of the $\alpha_v\beta_3$ integrin expression (9–11, 42). Peptides labeled with minimum structural alteration, peptide carbohydrate conjugates and peptidomimetics, as well as homodimeric and homomultimeric ligand systems are being evaluated (43, 44). The most promising monomeric ligand, [^{18}F]Galacto-RGD (Fig. 7), has been optimized by carbohydration and shows decreased nonspecific binding and improved excretion kinetics compared with the nonglycosylated reference compound. [^{18}F]Galacto-RGD has been successfully evaluated in clinical studies in patients suffering from malignant melanomas, sarcomas, head and neck cancer, glioblastomas, and breast cancer (10, 11, 45, 46). Standard uptake values in tumors ranged from 1.2 to 9.0. Tumor-to-blood and tumor-to-muscle ratios increased over time, with peak ratios of approximately 3 and 8 at 70 min after injection. The tumor kinetics was consistent with a two-tissue compartment model with reversible specific binding. Thus, this tracer offers a new strategy for noninvasive monitoring of molecular processes that may provide useful information for planning and guiding of therapeutic approaches targeting the $\alpha_v\beta_3$ integrin.

Apoptosis. Molecular imaging of phosphatidylserine by Annexin V or AFIM, a small 9-kDa domain of Annexin V engineered by mutagenesis, has major limitations. (*a*) Phosphatidylserine is only available "during" the apoptotic process of the cell, and thus, this target is "presented" only for a few hours. Due to the small time window, the effective concentration of available apoptotic cells is correspondingly low. (*b*) Tumors often exhibit both rapid cell growth and apoptosis, thus leading to a considerable background level of phosphatidylserine presentation in the steady state (47, 48).

Initial reports on the imaging of apoptosis by caspase inhibitors revealed low specific uptake of the compounds (31). This corroborates the rule of thumb that enzyme inhibitors, in contrast to enzyme substrates, are poor tracers (inhibitors bind to the enzyme in a 1:1 ratio, whereas the accumulation of an enzyme substrate is amplified). It is

worthwhile to reiterate that only in a few cases, where the target is expressed at a high density (e.g., imaging of ^{11}C-β-hydroxylase in adrenal cortical tumors using the inhibitor metomidate), is the imaging of an enzyme successful using a radiolabeled inhibitor.

To increase the cellular uptake and thus availability of the tracer at the target site, caspase substrates were conjugated to Tat peptides (nonspecific membrane-transducing peptides derived from the coat of the HIV). Among the tested compounds, Tat(49-57)-yDEVDG-NH_2 and Tat(57-49)-yDEVDG-NH_2 were favorably taken up by apoptotic cells compared with that of controls (30). Nevertheless, further optimization is necessary to achieve a relevant accumulation of the labeled fragments after proteolytic cleavage.

Promising small-molecule apoptosis markers have recently been developed. One of these compounds, Zn^{2+}-dipicolylamine, binds phosphatidylserine-rich membranes in a Ca^{2+}-independent manner and could be a very useful reagent for detecting apoptosis (49, 50). In addition, a novel family of low molecular weight compounds based on sulfonamides (ApoSense molecules) has been developed (42, 51, 52). Remarkably, these compounds showed selective passage through the membrane and accumulation within the cytoplasm of apoptotic cells. Although it remains to be shown, the mechanism hypothesized is that these compounds may bind to phosphatidylcholine and subsequently be transported into the cells during activation of scramblases. If no scramblases are activated, the loose complex dissociates and the sulfonamide leaves the cell membrane, thereby promoting clearance. Sulfonamides may therefore represent a novel class of small-molecule probes of potential value for *in vivo* imaging of apoptosis.

Receptor expression. Epidermal growth factor receptor tyrosine kinase is overexpressed on more than two thirds of human cancers (53–55). Two first-generation receptor ligands developed for PET imaging, [^{18}F]MLO1 (reversible inhibitor) and [^{11}C]MLO3 (irreversible inhibitor), showed good binding characteristics and inhibitory activities but were found to have unsuitable *in vivo* pharmacokinetics due to a rapid washout from the tumor and rapid *in vivo* degradation, respectively (53). Newly optimized ^{11}C-labeled analogues with improved *in vivo* stability and retained binding and inhibitory characteristics were developed and seem promising candidates for visualization of epidermal growth factor receptor–overexpressing tumors (54). The ^{11}C labeling of another reversible epidermal growth factor receptor tyrosine kinase inhibitor, Iressa, has been reported (55), highlighting the potential effect for imaging this target.

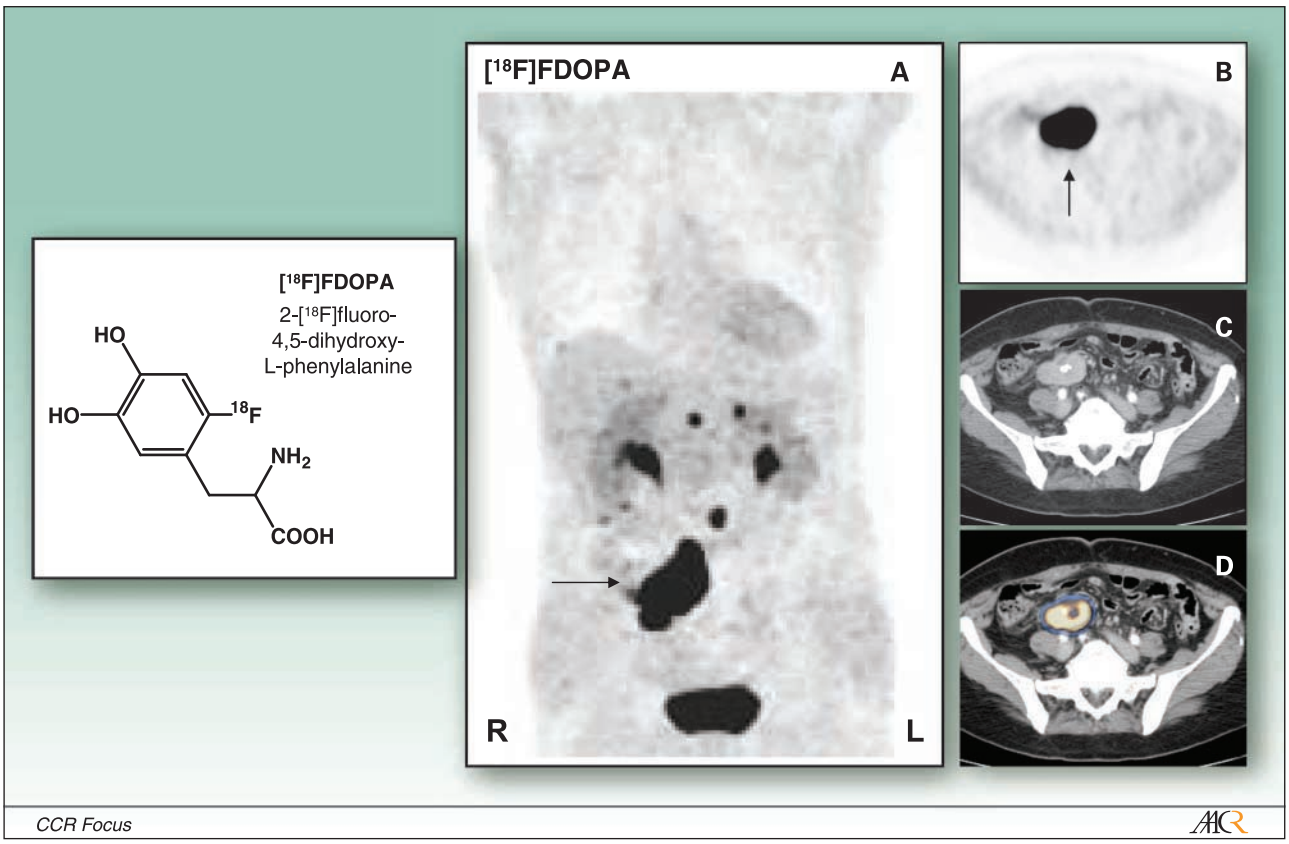

Fig. 5. [^{18}F]FDOPA. [^{18}F]FDOPA-PET/CT of a patient with neuroendocrine carcinoma. Intense focal tracer uptake in the primary tumor (*arrow*) and multiple lymph node and liver metastases are seen. *A,* maximum intensity projection of [^{18}F]FDOPA-PET. *B,* transaxial section of [^{18}F]FDOPA-PET. *C,* corresponding transaxial section of CT. *D,* fused image ([^{18}F]FDOPA-PET/CT). Transaxial sections indicate the primary tumor (PET images kindly provided by Dr. S. Reske).

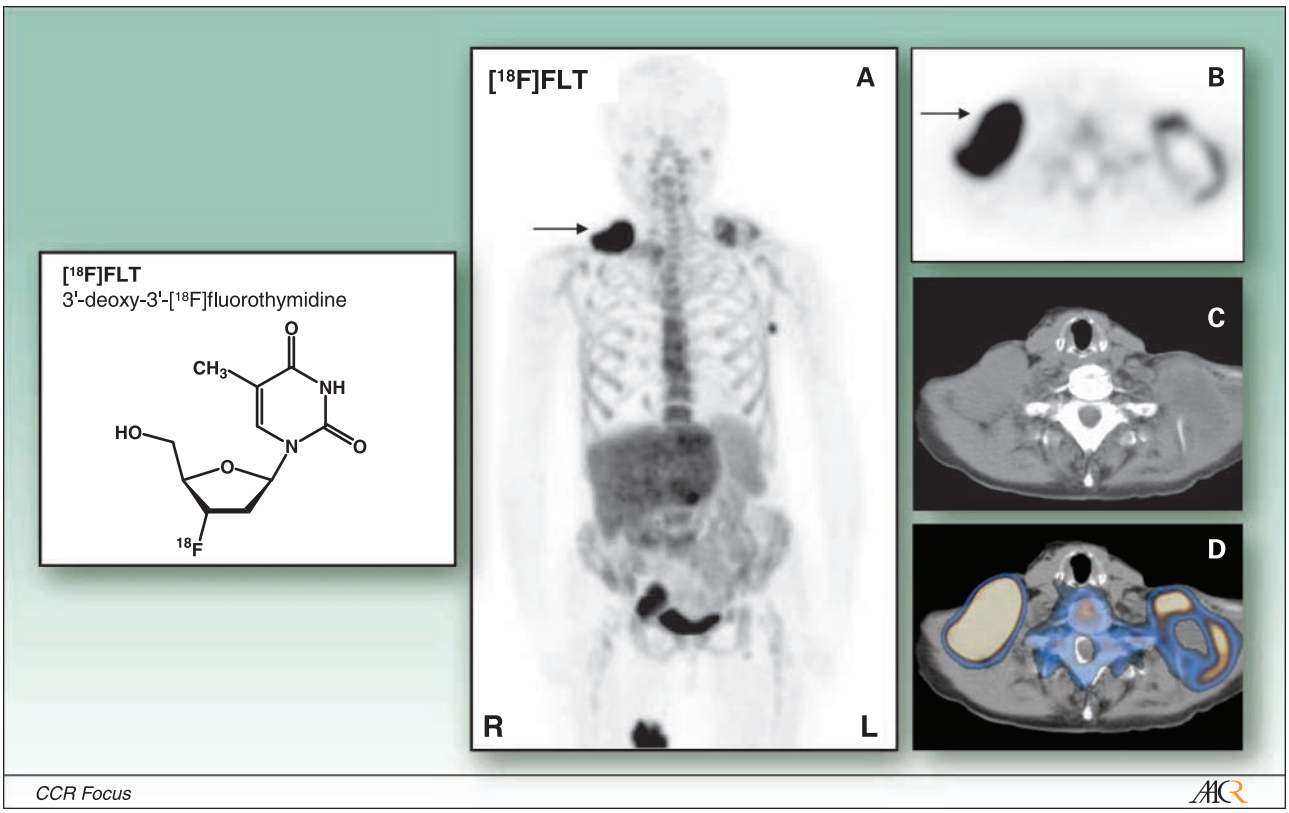

Fig. 6. [^{18}F]FLT. [^{18}F]FLT-PET/CT of a patient with aggressive non – Hodgkin's lymphoma. Intense focal tracer uptake can be observed in sites of lymphoma involvement, including sites at the right supraclavicular region, left axilla, and right femoral region. Medium intense uptake in the tumor margin of a lesion at the left shoulder region. *A,* maximum intensity projection of [^{18}F]FLT-PET. *B,* transaxial section of [^{18}F]FLT-PET. *C,* corresponding transaxial section of CT. *D,* fused image ([^{18}F]FLT-PET/CT; PET images kindly provided by Dr. S. Reske).

One important issue in the search for new imaging targets is the thorough assessment of the clinical relevance of a potential target. For example, a variety of receptors for regulatory peptides, such as somatostatin, gastrin, bombesin, gastrin-releasing peptide, neurotensin, or neuropeptide Y, are overexpressed on tumors (56). Currently, only the somatostatin receptor system has been fully exploited, leading to the development of highly optimized radiolabeled somatostatin receptor ligands (57), for example, [^{68}Ga]DOTA-D-Phe^{1}-Tyr^{3}-octreotide (Fig. 8). For most other neuropeptide receptor systems, there are still open issues to be addressed. This may require a further optimization of the radioligands and determination of the level of receptor expression and its distribution in tissues. Reubi and Waser have undertaken the task to thoroughly map a large number of tumor specimens and normal tissues for their neuropeptide receptor expression, which, hand in hand with the development of suitable receptor radioligands, constitutes the basis of successful clinical receptor imaging. This strategy also opens perspectives for efficient multireceptor targeting (58).

Another rule of thumb, receptor agonists have been assumed to be more suitable tracers than antagonists. Due to the internalization of the receptor-agonists complex, intracellular accumulation of the ligand in endosomal and finally lysosomal compartments can occur and usually results in high target-to-background ratios. Thus, radiolabeled antagonists, lacking the ability of receptor-mediated internalization, have not been regarded as promising tracers in oncology despite their success in imaging targets in the central nervous system. However, very recently, high tumor uptake and long retention of a somatostatin receptor–selective peptide antagonists has been shown in mice recently, reaching 60% of the injected dose per gram tumor at 1 h after injection and remaining at this considerably high level for up to 72 h (59). *In vitro* studies revealed that the antagonists labeled a higher number of binding sites than the agonists tested. If this observation can be confirmed for other receptor systems, the use of radiolabeled antagonists may considerably improve the sensitivity of receptor-targeted imaging.

Hypoxia. The major clinical relevance of tumor hypoxia lies in its negative predictive value for local tumor progression, the likeliness of metastasis, and for overall prognosis. In addition, tumor cell hypoxia has a negative effect on anticancer treatment, as hypoxic cells are two to three times more resistant to a single fraction of ionizing radiation compared with cells with normal oxygenation levels. Intensity-modulated radiation therapy allows selective dose escalation in hypoxic tumor regions. However, its applicability relies on the success of imaging to identify the volume of tumor tissue hypoxia.

To date, there are two distinct approaches for noninvasive *in vivo* quantification of the partial oxygen pressure by radiotracer imaging. One is based on the intracellular retention of nitroimidazoles (60, 61), such as [^{18}F]fluoromisonidazole or [^{18}F]fluoroazomycin arabinoside (FAZA; Fig. 9; ref. 62), following transmembrane diffusion and reduction to a radical form by ubiquitous nitroreductases. Under hypoxic conditions, these radicals cannot be reoxidized, which results in a binding to intracellular macromolecules, preventing back diffusion across the cell membrane. A subtle adjustment of the redox potential is a prerequisite for these tracers.

In contrast to nitroimidazole compounds, the exact targeting and retention mechanism of [^{60,62,64}Cu]diacetyl-bis-N_4-methylthiosemicarbazone (Cu-ATSM) is not completely understood. The reduction of Cu(II) to Cu(I) has been identified as the crucial step (63–65), and recently, the presence of cellular copper exporters (ATP7A and ATP7B) has been suggested to be responsible for a fast washout of copper isotopes from hypoxic tissue (66, 67).

Metastasis. Recently, chemokine receptors have been found to play a major role in the regulation of tumor metastasis and homing. Among those receptors, the chemokine receptor CXCR4 is highly expressed in a variety of tumors. Both the expression of CXCR4 and of its endogenous ligand, the stromal cell-derived factor-1α, are up-regulated during hypoxia. It has been shown that activation of CXCR4 leads to targeted metastasis by homing of circulating tumor cells to organs that express stromal cell-derived factor-1α, such as bone marrow, lung, and liver. Recently, a radiolabeled cyclic pentapeptide antagonist has been developed, and quantification of CXCR4 receptor expression has been investigated in animal models (68). Detailed studies need to show whether the physiologic expression pattern of CXCR4 correlates with the mobilization and homing of hematopoietic stem cells and if progenitor cells may interfere with imaging of metastasis.

Reevaluation of existing tracers/targets. On some occasions, a reevaluation or a more detailed analysis of the molecular processes relevant for tracer accumulation is recommended. One example is [^{11}C]acetate, which was initially introduced for imaging oxidative metabolism in the heart. More recently, [^{11}C]acetate was suggested for imaging of prostate cancer. Similar to radiolabeled choline, but not investigated in great detail, [^{11}C]acetate is taken up in cells with an enhanced lipid synthesis rate. Recently, it has been shown that [^{14}C]acetate is incorporated in the cellular lipid pool of tumor cells (69). The key enzyme in fatty acid synthesis, fatty acid synthase, has been found to be highly overexpressed in a variety of tumors, such as mammary cancer, gastrointestinal stromal tumors, or prostate cancer. Consequently, it has been hypothesized that [^{11}C]acetate may serve as a substrate for fatty acid synthase. It

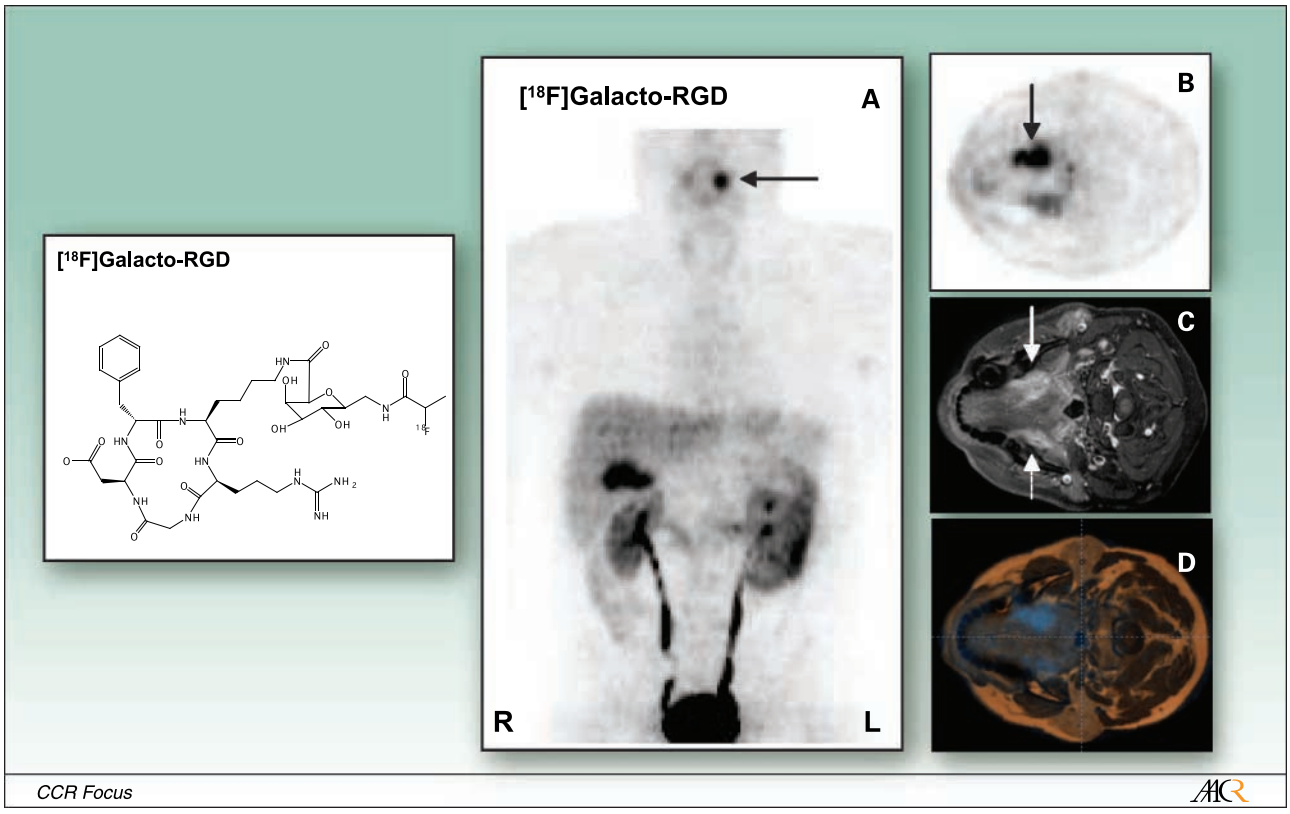

Fig. 7. [^{18}F]Galacto-RGD. Arrows, [^{18}F]Galacto-RGD-PET and magnetic resonance tomography of a patient with a squamous cell carcinoma. Physiologic uptake in the spleen and predominantly renal excretion of the tracer (kidney, ureter, and bladder). *A,* maximum intensity projection of [^{18}F]Galacto-RGD-PET. *B,* transaxial section of [^{18}F]Galacto-RGD-PET. *C,* T1 section with contrast enhancement of the corresponding magnetic resonance imaging scan. *D,* fused transaxial sections of [^{18}F]Galacto-RGD-PET and T1 section with contrast enhancement.

was shown that C75, a fatty acid inhibitor, completely inhibits the uptake of [^{3}H]acetate in PC-3 prostate cancer cells *in vitro*. Thus, although the [^{11}C]acetate-fatty acid synthase interaction has to be confirmed by *in vivo* imaging studies, especially with respect to the kinetics of the process, this example illustrates that only a detailed knowledge on the molecular trapping mechanism can provide insight into the potential for other applications.

What Kind of Tracer for Which Kind of Imaging?

The selection of a new target for a given disease, and thus the development of a new nuclear probe, is dependent on a sound molecular and cell biology information base (Fig. 2). For imaging in the context of planning of a chemotherapeutic intervention (e.g., is the therapeutic target expressed in high density?), and for therapy monitoring (does the applied dose of the therapeutic agent result in a sufficiently high target occupancy?), tracers with high specificity are required. Radiolabeled analogues of the corresponding therapeutic drugs seem to be the best initial imaging probes, but each drug would require its specific monitoring probe and infrastructure. Consequently, this costly strategy seems only applicable for imaging and therapy monitoring of some selected and often applied therapeutics.

For staging, response evaluation, and restaging the extent of the disease, the tracer uptake has to correlate with the therapeutic effect (biomarker) at all imaging time points (before and after therapy). Here, tracers with high sensitivity are required, allowing for the early assessment of therapeutic effects and response evaluation. Suitable probes for this kind of imaging address metabolic key processes, such as glucose utilization ([^{18}F]FDG) or cell proliferation ([^{18}F]FLT).

Conclusion

Apart from the continuing improvement in imaging equipment and technology, the success story of clinical molecular imaging is strongly dependent on the availability of powerful probes with optimal *in vivo* biodistribution and imaging characteristics. Three terms, (*a*) availability, (*b*) power or capability, and (*c*) *in vivo* characteristics, summarize the key features and problems in radiotracer development.

Availability includes radionuclide production, the development and technical realization of efficient and remote controlled syntheses, as well as regulatory issues and restrictions. Very few new approved radiopharmaceuticals have appeared in the last decade, and only a few tracers have any likelihood of approval in the near future. The clinical efficacy of a continuously increasing number of probes has already been

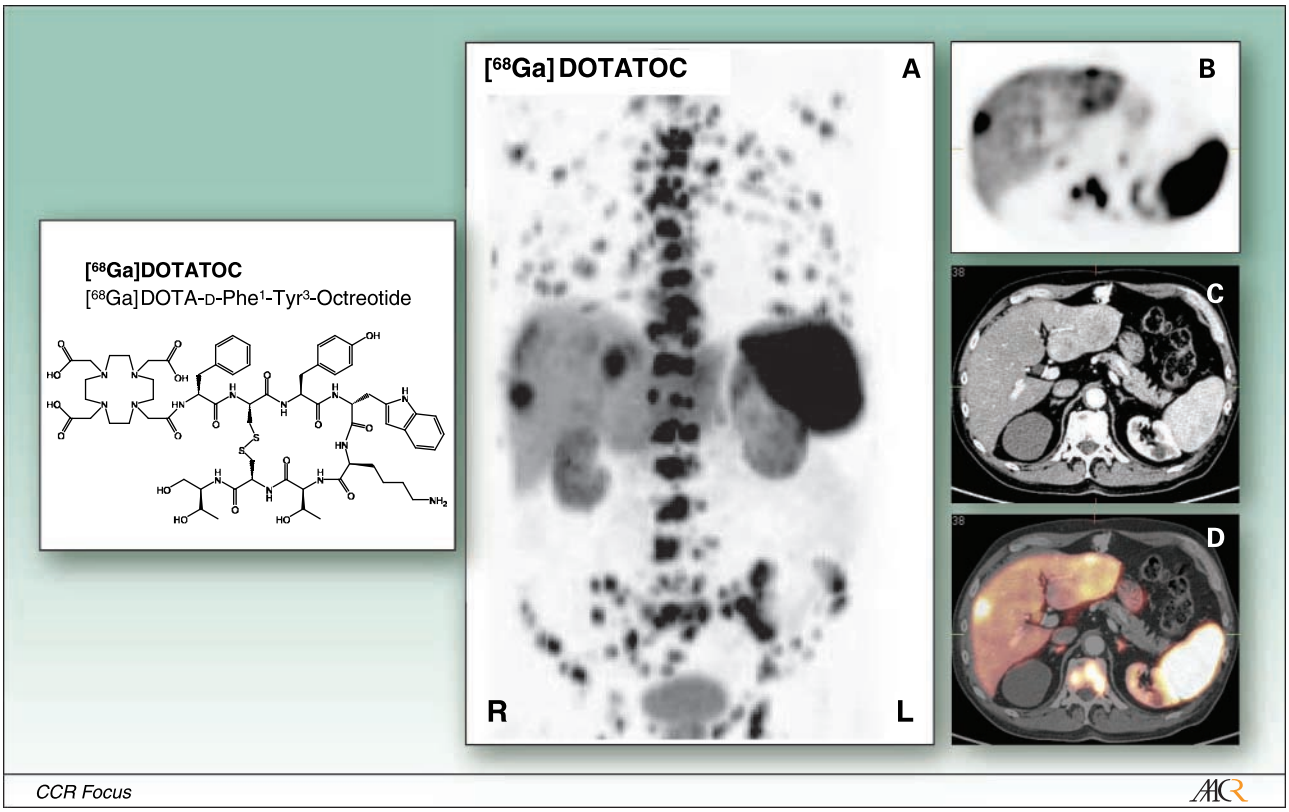

Fig. 8. [^{68}Ga]DOTATOC-PET/CT. [^{68}Ga]DOTATOC-PET/CT of a patient with neuroendocrine cancer and hepatic/osseous metastases. Multiple lesions with intense tracer uptake in somatostatin receptor 2–positive metastases of the liver, vertebral column, pelvis, scapula, and femur. *A,* maximum intensity projection of [^{68}Ga]DOTATOC-PET. *B,* transaxial section of [^{68}Ga]DOTATOC-PET. *C,* corresponding transaxial section of CT. *D,* fused image ([^{68}Ga]DOTATOC-PET/CT).

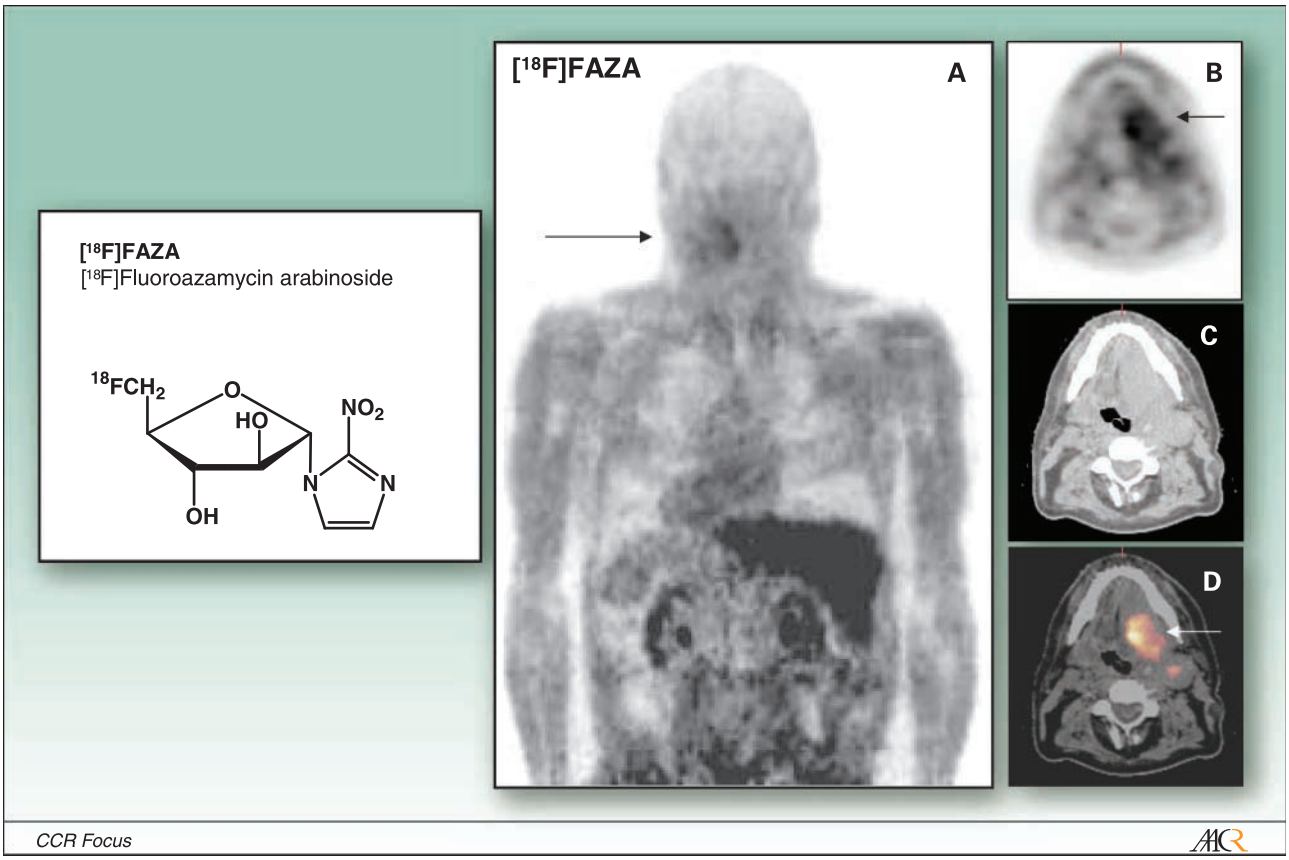

Fig. 9. [^{18}F]FAZA. Arrow, [^{18}F]FAZA-PET/CT of a patient with a squamous cell carcinoma in the head and neck. [^{18}F]FAZA accumulation indicates a hypoxic area in the tumor. *A,* maximum intensity projection of [^{18}F]FAZA-PET. *B,* transaxial section of [^{18}F]FAZA-PET. *C,* corresponding transaxial section of CT. *D,* fused image ([^{18}F]FAZA-PET/CT).

shown (e.g., [^{11}C]flumazenil and [^{11}C]methionine). Because ^{11}C probes (half-life of 20 min) are not feasible for commercial production and distribution, they must be produced locally by individual centers and will never reach a broad market.

The power or capability of a probe is predominantly determinated by a proper selection of the targets. Integration of genomic and proteomic information into the developmental process will improve and facilitate the selection of new targets with high relevance for therapy monitoring and prediction of therapy response.

The optimization of the "*in vivo* biodistribution and metabolism characteristics" of a molecular probe is potentially the most challenging task in the development of a new high-affinity radiolabeled ligand to image a specific endogenous molecular target. Catabolic stability, clearance rate, excretion route, specificity of uptake, accumulation, retention, etc. need to be properly adjusted and characterize the pharmacokinetic aspects of a "good *in vivo* probe." Radiopharmaceutical chemistry must strengthen the "pharmaceutical" component of new probe development. Finally, a "good *in vivo* probe" will only become a "good *in vivo* radiopharmaceutical" after it has been fully assessed in clinical trials.

Acknowledgments

We thank Drs. A. Buck, A. Beer, M. Souvatzoglou, and R. Blasberg for careful editorial assistance and Dr. S. Reske (Nuclear Medicine Clinic, Universitat Ulm, Ulm, Germany) for kindly providing some of the PET/CT images.

References

1. Blasberg R. Imaging update: new windows, new views. Clin Cancer Res 2007;13:3444–8.
2. Mankoff DA, Eary JF, Link JM, et al. Tumor-specific PET imaging in patients: FDG and beyond. Clin Cancer Res 2007;13:3660–9.
3. Liu ET. Expression genomics and drug development: towards predictive pharmacology. Brief Funct Genomic Proteomic 2005;3:303–21.
4. Bild AH, Potti A, Nevins JR. Linking oncogenic pathways with therapeutic opportunities. Nat Rev Cancer 2006;6:735–41.
5. Hofmann M, Maecke H, Borner R, et al. Biokinetics and imaging with the somatostatin receptor PET radioligand (68)Ga-DOTATOC: preliminary data. Eur J Nucl Med 2001;28:1751–7.
6. Maecke HR, Hofmann M, Haberkorn U. (68)Ga-labeled peptides in tumor imaging. J Nucl Med 2005;46:172–8S.
7. Wester HJ, Schottelius M, Scheidhauer K, et al. PET imaging of somatostatin receptors: design, synthesis and preclinical evaluation of a novel ^{18}F-labelled, carbohydrated analogue of octreotide. Eur J Nucl Med Mol Imaging 2003;30:117–22.
8. Meisetschlager G, Poethko T, Stahl A, et al.

Gluc-Lys([^{18}F]FP)-TOCA PET in patients with SSTR-positive tumors: biodistribution and diagnostic evaluation compared with [111In]DTPA-octreotide. J Nucl Med 2006;47:566–73.

9. Haubner R, Wester HJ, Weber WA, et al. Noninvasive imaging of $\alpha(v)\beta_3$ integrin expression using ^{18}F-labeled RGD-containing glycopeptide and positron emission tomography. Cancer Res 2001;61:1781–5.

10. Haubner R, Weber WA, Beer AJ, et al. Noninvasive visualization of the activated $\alpha_v\beta_3$ integrin in cancer patients by positron emission tomography and [^{18}F]Galacto-RGD. PLoS Med 2005;2:244–52.

11. Beer AJ, Haubner R, Sarbia M, et al. Positron emission tomography using [^{18}F]Galacto-RGD identifies the level of integrin $\alpha(v)\beta_3$ expression in man. Clin Cancer Res 2006;12:3942–9.

12. Holliger P, Hudson PJ. Engineered antibody fragments and the rise of single domains. Nat Biotechnol 2005;23:1126–36.

13. Smith-Jones PM, Solit DB, Akhurst T, Afroze F, Rosen N, Larson SM. Imaging the pharmacodynamics of HER2 degradation in response to Hsp90 inhibitors. Nat Biotechnol 2004;22:701–6.

14. McGuire AH, Dehdashti F, Siegel BA, et al. Positron tomographic assessment of 16 α-[^{18}F] fluoro-17 β-estradiol uptake in metastatic breast carcinoma. J Nucl Med 1991;32:1526–31.

15. Eubank WB, Mankoff DA. Current and future uses of positron emission tomography in breast cancer imaging. Semin Nucl Med 2004;34:224–40.

16. Wester HJ, Herz M, Weber W, et al. Synthesis and radiopharmacology of *O*-(2-[^{18}F]fluoroethyl)-L-tyrosine for tumor imaging. J Nucl Med 1999;40:205–12.

17. Weber WA, Wester HJ, Grosu AL, et al. *O*-(2-[^{18}F]fluoroethyl)-L-tyrosine and L-[methyl-^{11}C]methionine uptake in brain tumours: initial results of a comparative study. Eur J Nucl Med 2000;27:542–9.

18. Pauleit D, Zimmermann A, Stoffels G, et al. ^{18}F-FET PET compared with ^{18}F-FDG PET and CT in patients with head and neck cancer. J Nucl Med 2006;47:256–61.

19. Shields AF, Grierson JR, Dohmen BM, et al. Imaging proliferation *in vivo* with [F-18]FLT and positron emission tomography. Nat Med 1998;4:1334–6.

20. Wieder HA, Geinitz H, Rosenberg R, et al. PET imaging with [(18)F]3′-deoxy-3′-fluorothymidine for prediction of response to neoadjuvant treatment in patients with rectal cancer. Eur J Nucl Med Mol Imaging. Epub 2006 Dec 29.

21. Picchio M, Treiber U, Beer AJ, et al. Value of ^{11}C-choline PET and contrast-enhanced CT for staging of bladder cancer: correlation with histopathologic findings. J Nucl Med 2006;47:938–44.

22. Reske SN, Blumstein NM, Neumaier B, et al. Imaging prostate cancer with ^{11}C-choline PET/CT. J Nucl Med 2006;47:1249–54.

23. DeGrado TR, Coleman RE, Wang S, et al. Synthesis and evaluation of ^{18}F-labeled choline as an oncologic tracer for positron emission tomography: initial findings in prostate cancer. Cancer Res 2001;61:110–7.

24. Price DT, Coleman RE, Liao RP, Robertson CN, Polascik TJ, DeGrado TR. Comparison of [^{18}F]fluorocholine and [^{18}F]fluorodeoxyglucose for positron emission tomography of androgen dependent and androgen independent prostate cancer. J Urol 2002;168:273–80.

25. Koopmans KP, de Vries EG, Kema IP, et al. Staging of carcinoid tumours with ^{18}F-DOPA PET: a prospective, diagnostic accuracy study. Lancet Oncol 2006;7:728–34.

26. Yaghoubi SS, Wu L, Liang Q, et al. Direct correlation between positron emission tomographic images of two reporter genes delivered by two distinct adenoviral vectors. Gene Ther 2001;8:1072–80.

27. Jacobs AH, Rueger MA, Winkeler A, et al. Imaging-guided gene therapy of experimental gliomas. Cancer Res 2007;67:1706–15.

28. Sodee DB, Ellis RJ, Samuels MA, et al. Prostate cancer and prostate bed SPECT imaging with ProstaScint: semiquantitative correlation with prostatic biopsy results. Prostate 1998;37:140–8.

29. Wagner S, Breyholz HJ, Faust A, et al. Molecular imaging of matrix metalloproteinases *in vivo* using small molecule inhibitors for SPECT and PET. Curr Med Chem 2006;13:2819–38.

30. Bauer C, Bauder-Wuest U, Mier W, Haberkorn U, Eisenhut M. ^{131}I-labeled peptides as caspase substrates for apoptosis imaging. J Nucl Med 2005;46:1066–74.

31. Haberkorn U, Kinscherf R, Krammer PH, Mier W, Eisenhut M. Investigation of a potential scintigraphic marker of apoptosis: radioiodinated Z-Val-Ala-DL-Asp(O-methyl)-fluoromethyl ketone. Nucl Med Biol 2001;28:793–8.

32. Kopka K, Faust A, Keul P, et al. 5-Pyrrolidinylsulfonyl isatins as a potential tool for the molecular imaging of caspases in apoptosis. J Med Chem 2006;49:6704–15.

33. Buck AK, Schirrmeister H, Hetzel M, et al. 3-Deoxy-3-[(18)F]fluorothymidine-positron emission tomography for noninvasive assessment of proliferation in pulmonary nodules. Cancer Res 2002;62:3331–4.

34. Buck AK, Bommer M, Stilgenbauer S, et al. Molecular imaging of proliferation in malignant lymphoma. Cancer Res 2006;66:11055–61.

35. Buck AK, Halter G, Schirrmeister H, et al. Imaging proliferation in lung tumors with PET: ^{18}F-FLT versus ^{18}F-FDG. J Nucl Med 2003;44:1426–31.

36. Sun H, Mangner TJ, Collins JM, Muzik O, Douglas K, Shields AF. Imaging DNA synthesis *in vivo* with ^{18}F-FMAU and PET. J Nucl Med 2005;46:292–6.

37. Haubner R, Wester HJ. Radiolabeled tracers for imaging of tumor angiogenesis and evaluation of anti-angiogenic therapies. Curr Pharm Des 2004;10:1439–55.

38. Miller JC, Pien HH, Sahani D, Sorensen AG, Thrall JH. Imaging angiogenesis: applications and potential for drug development. J Natl Cancer Inst 2005;97:172–87.

39. Berndorff D, Borkowski S, Moosmayer D, et al. Imaging of tumor angiogenesis using ^{99m}Tc-labeled human recombinant anti-ED-B fibronectin antibody fragments. J Nucl Med 2006;47:1707–16.

40. Demartis S, Tarli L, Borsi L, Zardi L, Neri D. Selective targeting of tumour neovasculature by a radiohalogenated human antibody fragment specific for the ED-B domain of fibronectin. Eur J Nucl Med 2001;28:534–9.

41. Santimaria M, Moscatelli G, Viale GL, et al. Immunoscintigraphic detection of the ED-B domain of fibronectin, a marker of angiogenesis, in patients with cancer. Clin Cancer Res 2003;9:571–9.

42. Haubner R. $\alpha(v)\beta(3)$-integrin imaging: a new approach to characterise angiogenesis? Eur J Nucl Med Mol Imaging 2006;33:54–63.

43. Poethko T, Schottelius M, Thumshirn G, et al. Two-step methodology for high-yield routine radiohalogenation of peptides: (18)F-labeled RGD and octreotide analogs. J Nucl Med 2004;45:892–902.

44. Thumshirn G, Hersel U, Goodman SL, Kessler H. Multimeric cyclic RGD peptides as potential tools for tumor targeting: solid-phase peptide synthesis and chemoselective oxime ligation. Chemistry 2003;9:2717–25.

45. Beer AJ, Haubner R, Wolf I, et al. PET-based human dosimetry of ^{18}F-galacto-RGD, a new radiotracer for imaging $\alpha_v\beta_3$ expression. J Nucl Med 2006;47:47:763–9.

46. Beer AJ, Haubner R, Goebel M, et al. Biodistribution and pharmacokinetics of the $\alpha_v\beta_3$-selective tracer ^{18}F-galacto-RGD in cancer patients. J Nucl Med 2005;46:1333–41.

47. Boersma HH, Kietselaer BL, Stolk LM, et al. Past, present, and future of annexin A5: from protein discovery to clinical applications. J Nucl Med 2005;46:2035–50.

48. Lahorte CM, Vanderheyden JL, Steinmetz N, Van de Wiele C, Dierckx RA, Slegers G. Apoptosis-detecting radioligands: current state of the art and future perspectives. Eur J Nucl Med Mol Imaging 2004;31:887–919.

49. Hanshaw RG, Smith BD. New reagents for phosphatidylserine recognition and detection of apoptosis. Bioorg Med Chem 2005;13:5035–42.

50. Hanshaw RG, Lakshmi C, Lambert TN, Johnson JR, Smith BD. Fluorescent detection of apoptotic cells by using zinc coordination complexes with a selective affinity for membrane surfaces enriched with phosphatidylserine. Chem Bio Chem 2005;6:2214–20.

51. Damianovich M, Ziv I, Heyman SN, et al. ApoSense: a novel technology for functional molecular imaging of cell death in models of acute renal tubular necrosis. Eur J Nucl Med Mol Imaging 2006;33:281–91.

52. Aloya R, Shirvan A, Grimberg H, et al. Molecular imaging of cell death *in vivo* by a novel small molecule probe. Apoptosis 2006;11:2089–101.

53. Shaul M, Abourbeh G, Jacobson O, et al. Novel iodine-124 labeled EGFR inhibitors as potential PET agents for molecular imaging in cancer. Bioorg Med Chem 2004;12:3421–9.

54. Mishani E, Abourbeh G, Jacobson O, et al. High-affinity epidermal growth factor receptor (EGFR) irreversible inhibitors with diminished chemical reactivities as positron emission tomography (PET)-imaging agent candidates of EGFR overexpressing tumors. J Med Chem 2005;48:5337–48.

55. Wang JQ, Gao M, Miller KD, Sledge GW, Zheng QH. Synthesis of [^{11}C]Iressa as a new potential PET cancer imaging agent for epidermal growth factor receptor tyrosine kinase. Bioorg Med Chem Lett 2006;16:4102–6.

56. Reubi JC. Peptide receptors as molecular targets for cancer diagnosis and therapy. Endocr Rev 2003;24:389–427.

57. Eberle AN, Mild G, Froidevaux S. Receptor-mediated tumor targeting with radiopeptides. Part 1. General concepts and methods: applications to somatostatin receptor-expressing tumors. J Recept Signal Transduct Res 2004;24:319–455.

58. Reubi JC, Waser B. Concomitant expression of several peptide receptors in neuroendocrine tumours: molecular basis for *in vivo* multireceptor tumour targeting. Eur J Nucl Med Mol Imaging 2003;30:781–93.

59. Ginj M, Zhang H, Waser B, et al. Radiolabeled somatostatin receptor antagonists are preferable to agonists for *in vivo* peptide receptor targeting of tumors. Proc Natl Acad Sci U S A 2006;103:16436–41.

60. Padhani AR. Where are we with imaging oxygenation in human tumours? Cancer Imaging 2005;28:128–30.

61. Padhani AR, Krohn KA, Lewis JS, Alber M. Imaging oxygenation of human tumours. Eur Radiol 2007;17:861–72.

62. Piert M, Machulla HJ, Picchio M, et al. Hypoxia-specific tumor imaging with ^{18}F-fluoroazomycin arabinoside. J Nucl Med 2005;46:106–13.

63. Dehdashti F, Mintun MA, Lewis JS, et al. *In vivo* assessment of tumor hypoxia in lung cancer with ^{60}Cu-ATSM. Eur J Nucl Med Mol Imaging 2003;30:844–50.

64. Dehdashti F, Grigsby PW, Mintun MA, Lewis JS,

Siegel BA, Welch MJ. Assessing tumor hypoxia in cervical cancer by positron emission tomography with ^{60}Cu-ATSM: relationship to therapeutic response—a preliminary report. Int J Radiat Oncol Biol Phys 2003; 55:1233–8.

65. Lewis JS, Sharp TL, Laforest R, Fujibayashi Y, Welch MJ. Tumor uptake of copper-diacetyl-bis(*N*(4)-methylthiosemicarbazone): effect of changes in tissue oxygenation. J Nucl Med 2001; 42:655–61.

66. Burgman P, O'Donoghue JA, Lewis JS, Welch MJ, Humm JL, Ling CC. Cell line-dependent differences in uptake and retention of the hypoxia-selective nuclear imaging agent Cu-ATSM. Nucl Med Biol 2005;32: 623–30.

67. O'Donoghue JA, Zanzonico P, Pugachev A, et al. Assessment of regional tumor hypoxia using ^{18}F-fluoromisonidazole and 64 Cu(II)-diacetyl-bis (N^4-methylthiosemicarbazone) positron emission tomography: comparative study featuring microPET imaging, Po2 probe measurement, autoradiography, and fluorescent microscopy in the R3327-AT and FaDu rat tumor models. Int J Radiat Oncol Biol Phys 2005;61:1493–502.

68. Koglin N, Anton M, Hauser A, et al. CXCR4 chemokine receptor SPECT/PET imaging with radiolabeled CPCR4: a promising approach for imaging metastatic processes. J Nucl Med 2006;47:505p.

69. Swinnen JV, van Veldhoven PP, Timmermans L, et al. Fatty acid synthase drives the synthesis of phospholipids partitioning into detergent-resistant membrane microdomains. Biochem Biophys Res Commun 2003;302:898–903.